AD-A153 135 CRITICAL CONDITIONS FOR FAILURE IN MATERIALS SUBJECTED TO HIGH RATES OF L..(U) BROWN UNIV PROVIDENCE RI DIV OF ENGINEERING R J CLIFTON ET AL. 20 MAR 85 1/1

UNCLASSIFIED ARO-18414.18-EG DAAG29-81-K-0121 F/G 20/11 NL

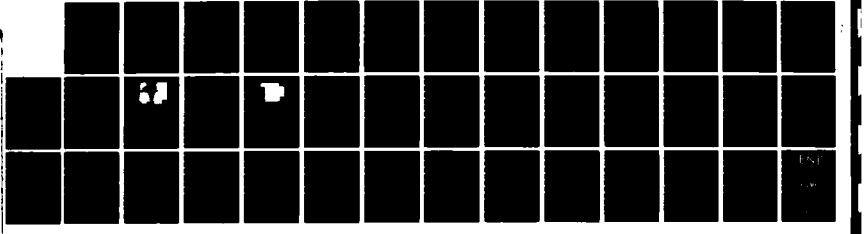

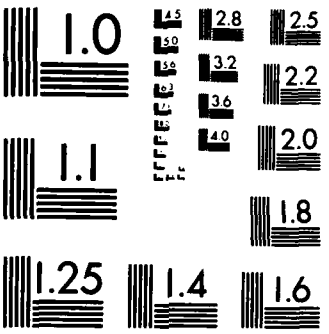

MICROCOPY RESOLUTION TEST CHART
NATIONAL BUREAU OF STANDARDS-1963-A

REPORT DOCUMENTATION PAGE

READ INSTRUCTIONS BEFORE COMPLETING FORM

1. REPORT NUMBER: ARO 18414.18-EG	2. GOVT ACCESSION NO.: N/A
3. RECIPIENT'S CATALOG NUMBER: N/A	
4. TITLE (and Subtitle): Critical Conditions for Failure in Materials Subjected to High Rates of Loading	5. TYPE OF REPORT & PERIOD COVERED: FINAL Aug. 15 1981 - Nov. 30, 1984
	6. PERFORMING ORG. REPORT NUMBER
7. AUTHOR(s): R.J. Clifton	8. CONTRACT OR GRANT NUMBER(s): DAAG29-81-K-0121
PERFORMING ORGANIZATION NAME AND ADDRESS: Division of Engineering, Brown University, Providence, RI 02912	10. PROGRAM ELEMENT, PROJECT, TASK AREA & WORK UNIT NUMBERS
CONTROLLING OFFICE NAME AND ADDRESS: U. S. Army Research Office, Post Office Box 12211, Research Triangle Park, NC 27709	12. REPORT DATE: March 20, 1985
	13. NUMBER OF PAGES: 36
MONITORING AGENCY NAME & ADDRESS (if different from Controlling Office)	15. SECURITY CLASS. (of this report): Unclassified
	15a. DECLASSIFICATION/DOWNGRADING SCHEDULE

DISTRIBUTION STATEMENT (of this Report)

Approved for public release; distribution unlimited.

17. DISTRIBUTION STATEMENT (of the abstract entered in Block 20, if different from Report)

NA

18. SUPPLEMENTARY NOTES

The view, opinions, and/or findings contained in this report are those of the author(s) and should not be construed as an official Department of the Army position, policy, or decision, unless so designated by other documentation.

19. KEY WORDS (Continue on reverse side if necessary and identify by block number)

Dynamic plasticity, shear bands, fracture initiation, ductile fracture, adiabatic shear, AISI 4340 VAR steel, AISI 1020 steel, dynamic fracture, strain-rate sensitivity, thermal softening

20. ABSTRACT (Continue on reverse side if necessary and identify by block number)

Mechanisms of the plastic deformation and failure of steels under dynamic loading conditions have been examined through investigations in three areas: dynamic plasticity, shear bands, and fracture initiation. The dynamic plastic response of 4340 VAR steel has been measured in torsion experiments at strain rates from 10^{-4} sec^{-1} to 10^{4} sec^{-1} and in pressure-shear experiments at strain rates of 10^{5} sec^{-1}. Torsion experiments were conducted at temperatures from -190C to 23C on three tempers (HRC 55, 44, 33). Relatively weak strain-rate

sensitivity obtained in these experiments has been related to the high athermal stress barrier that must be overcome for plastic deformation at low temperatures. Even at strain rates of 10^5 sec^{-1} the flow stress is less than the quasi-static yield stress extrapolated to 0^oK.

Critical conditions for shear band formation were investigated in dynamic torsion experiments on four steels. Temperature profiles in the vicinity of the shear bands were measured using a ten-element, infrared detector system. Numerical simulations were used to assess the roles of strain hardening, strain-rate sensitivity, thermal softening and heat conduction on shear band formation. Finite element methods were developed for rate dependent plasticity and applied to calculations of failure through shear band propagation and ductile fracture. From these various investigations a reasonably coherent understanding of shear band formation appears to be emerging. At high strain rates, thermal softening can offset strain hardening and allow shear strain localization to begin. If strain-rate sensitivity is relatively weak, then a strong instability can develop. Interaction of stress fields of neighboring shear bands has a strong influence on the propagation of the bands.

The effects of microstructure on dynamic and quasi-static fracture initiation of AISI 1020 steel were investigated by means of our notched-round bar experiment. The results cover the temperature range -150C to 100C. For static loading under ductile conditions the results are now being supplemented by a detailed study to determine the instant of fracture initiation. A new plate impact experiment was developed for studying fracture of pre-cracked plates at ultra-high loading rates.

FINAL REPORT

CRITICAL CONDITIONS FOR FAILURE IN MATERIALS SUBJECTED TO HIGH RATES OF LOADING

ARO PROPOSAL NUMBER P-18414-E

GRANT NUMBER DAAG29-81-K-0121

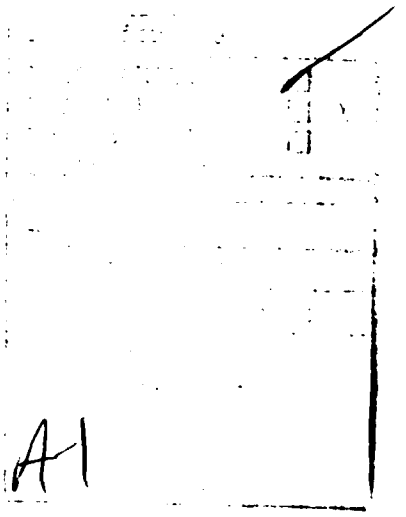

BROWN UNIVERSITY

PROVIDENCE, RI 02912

MARCH, 1985

R.J. Clifton
R.J. Asaro
J. Duffy
L.B. Freund
A. Needleman

Abstract

Mechanisms of the plastic deformation and failure of steels under dynamic loading conditions have been examined through investigations in three areas: dynamic plasticity, shear bands, and fracture initiation. The dynamic plastic response of 4340 VAR steel has been measured in torsion experiments at strain rates from 10^{-4} sec^{-1} to 10^{4} sec^{-1} and in pressure-shear experiments at strain rates of 10^{5} sec^{-1}. Torsion experiments were conducted at temperatures from -190C to 23C on three tempers (HRC 55, 44, 33). Relatively weak strain-rate sensitivity obtained in these experiments has been related to the high athermal stress barrier that must be overcome for plastic deformation at low temperatures. Even at strain rates of 10^{5} sec^{-1} the flow stress is less than the quasi-static yield stress extrapolated to $0^{o}K$.

Critical conditions for shear band formation were investigated in dynamic torsion experiments on four steels. Temperature profiles in the vicinity of the shear bands were measured using a ten-element, infrared detector system. Numerical simulations were used to assess the roles of strain hardening, strain-rate sensitivity, thermal softening and heat conduction on shear band formation. Finite element methods were developed for rate dependent plasticity and applied to calculations of failure through shear band propagation and ductile fracture. From these various investigations a reasonably coherent understanding of shear band formation appears to be emerging. At high strain rates, thermal softening can offset strain hardening and allow shear strain localization to begin. If strain-rate sensitivity is relatively weak, then a strong instability can develop. Interaction of stress fields of neighboring shear bands has a strong influence on the propagation of the bands.

The effects of microstructure on dynamic and quasi-static fracture initiation of AISI 1020 steel were investigated by means of our notched-round bar experiment. The results cover the temperature range -150C to 100C. For static loading under ductile conditions the results are now being supplemented by a detailed study to determine the instant of fracture initiation. A new plate impact experiment was developed for studying fracture of pre-cracked plates at ultra-high loading rates.

1. PROBLEM STUDIED

This is the final report for an initial three-year funding of a major research program on the plastic deformation and failure of metals at high rates of loading. In this program, five faculty members with broad theoretical and experimental experience in solid mechanics and materials science have united their efforts in order to make significant advances in the understanding of the mechanisms of plastic deformation and fracture under dynamic conditions. Improved understanding of failure mechanisms is viewed as essential for obtaining improved descriptions of material behavior for implementation in computer codes used in the analysis and design of components subjected to dynamic loading. Furthermore, a more fundamental understanding of the mechanisms of failure is expected to lead to the design of improved microstructures for specific applications.

During the initial three years of this program the research group at Brown addressed three areas: dynamic plasticity, shear bands, and fracture initiation. In the dynamic plasticity investigations the experimental effort was directed towards understanding the temperature and strain-rate sensitivity of the flow stress in 4340 VAR steel. Dynamic torsion and pressure-shear impact experiments were used. A principal result of these experiments is that the flow stress increases with increasing strain rate, but there is no substantial increase in strain-rate sensitivity up to strain rates as high as $10^5\ s^{-1}$. Thus, it appears that the strain-rate sensitivity of 4340 VAR steel can be described adequately by elementary models.

In the shear band investigations, the roles of strain hardening, thermal softening and strain-rate sensitivity were demonstrated in analyses of a number of different model problems. All three of these material characteristics were found to be important in the development of shear bands at high rates of loading. Dynamic torsion experiments resulted in shear bands in four steels tested; large strains (greater than 100%) were necessary to obtain shear bands in a hot-rolled steel (AISI 1020). Temperatures as high as 450°C were measured using an infrared detector system which detects radiation from a spot size of approximately 20 μm. Higher temperatures are expected within transformation bands in which the widths are 5-10 μm. Analyses of shear band propagation have shown the importance of the interaction of shear bands.

In the fracture initiation investigations, the dependence of fracture toughness, and the relative fractions of fibrous and cleavage fracture areas on the microstructure, temperature, and loading rate was established for certain AISI 1020 steels with controlled microstructures. The experiments were performed in a notched bar configuration using both quasi-static and stress-wave loading. This fracture investigation was complemented by computer modeling of ductile fracture and by the development of a new plate impact experiment for studying dynamic fracture at ultra-high loading rates.

Research results obtained under the grant are described in more detail in the following section. References denoted by superscripts R, e.g. $(1984)^{R}$, are listed in Section 4; references without superscripts refer to publications, reports and theses that were supported by the grant and are listed in Section 3.

2. PRINCIPAL RESEARCH RESULTS

2.1 Dynamic Plasticity

2.1.1 Dynamic Torsion

A series of tests has been completed in which thin-walled tubular specimens of 4340 VAR steel have been tested in the torsional Kolsky (split-Hopkinson) bar (TANIMURA and DUFFY (1984)). These tests cover strain rates in shear from the quasi-static to about 10^3 s^{-1} and in a few instances, as high as 10^4 s^{-1}.

The heat treatment adopted for all 4340 VAR steel specimens tested in this project consists of: (1) normalizing at 900C for one hour, then cooling in argon; (2) austenitizing for one hour at 845C followed by an oil quench; and (3) temper for one hour at a prescribed temperature. Specimens were heat-treated in a dry argon atmosphere to avoid any oxidation. Tempers used were 200C, 425C and 600C. Cooling for the 200C temper was by an argon flow, while for the other two tempers it was through an oil-quench. In the particular case of the torsion specimens, the above times were reduced to half an hour due to the small size of the specimens. The resulting hardnesses were HRC 55, 44 and 33 respectively for the three tempers. Microscopic examination of the tempered specimens shows a martensitic microstructure with lath packets randomly oriented. The 425C and 600C microstructures are typical of a tempered martensite.

For all three tempers, experiments were conducted at four test temperatures: -190C, -120C, -50C and room temperature. In each case this included tests at quasi-static and dynamic strain rates, as well as tests in which either the temperature or the strain rate was changed rapidly from one constant value to another during the course of the deformation. These incremental experiments were performed in order to study temperature and strain rate history effects, i.e. to study the effects of a prestrain under one set of experimental conditions on the subsequent mechanical response under a different set of conditions.

Typical results of the quasi-static tests are shown in Figure 1, which

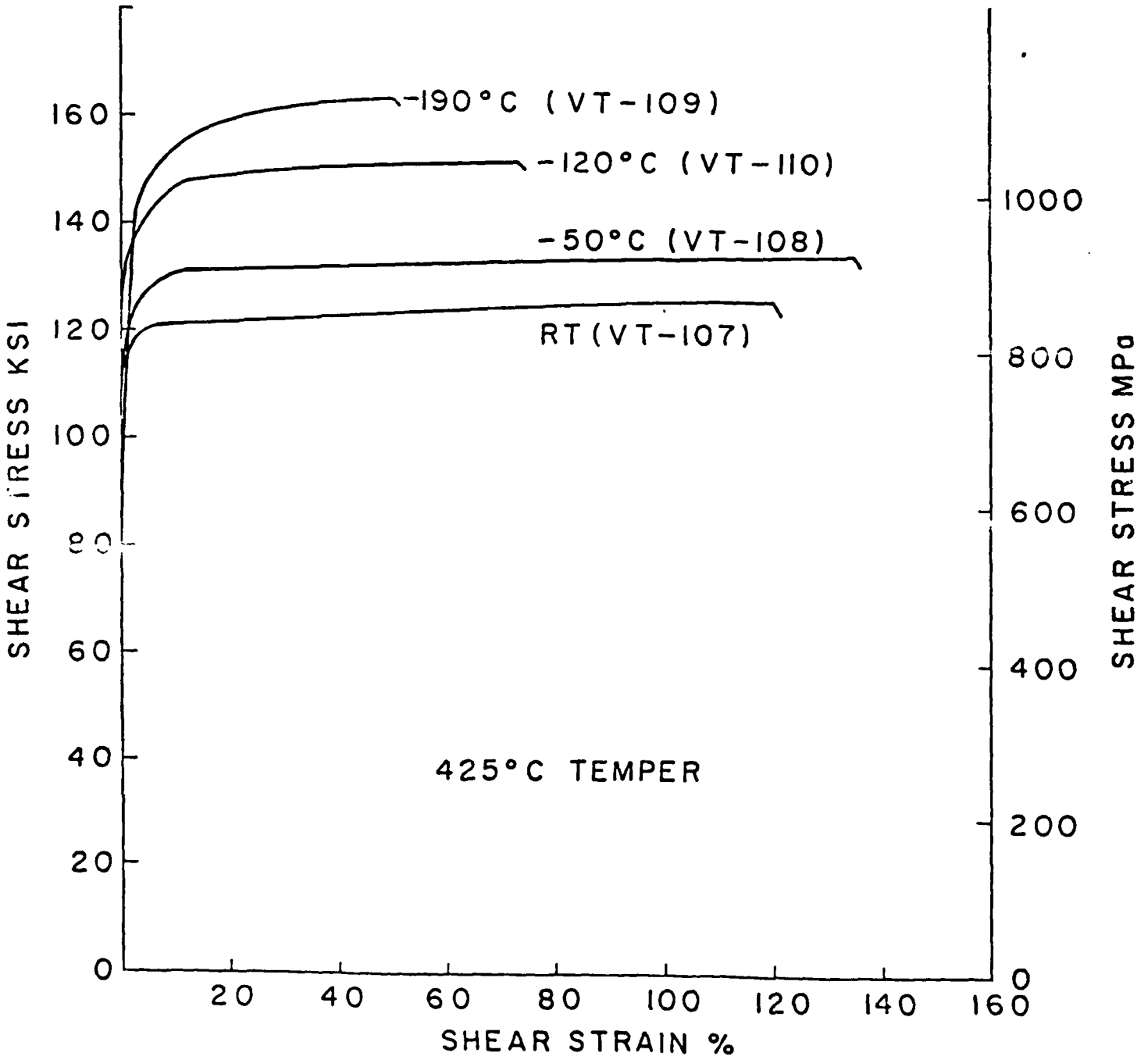

Fig. 1 Quasi-Static stress-strain curves of the 4340 VAR steel in the 425C Temper (HRC=44)

shows the stress-strain behavior in shear of the 425C temper at each of the four test temperatures. Each test was carried through until fracture. It is clear from the figure that the behavior of this steel is quite sensitive to test temperature and that the strain-hardening slope is quite small. Similar curves were obtained for the 600C temper and the 200C temper. For the 600C temper the stress level is lower while the temperature sensitivity is greater. For the 200C temper the stress attains a value of near 1600 MPa at -190C, but the temperature sensitivity is lower. As might be expected, the maximum shear strain before fracture is greatest for the 600C temper where it is 120% to 140%, while for the 200C temper fracture intervenes at a shear strain of about 15%. Generally, the temperature history effect is small; for instance, the stress-strain curve at -190C is substantially the same whether an early part of the straining occurs at -50C or at -190C. An exception occurs, however, for the 200C temper where a prestrain at -50C results in a higher stress level during subsequent deformation at -190C than would be obtained for deformation entirely at -190C. The history behavior of 4340 steel, including the 200C temper, is typical of that of the bcc metals and in particular of iron and steel; fcc and hcp metals show quite a different history effect, but the reasons for this difference are not clear (DUFFY (1983)).

Strain rate sensitivity in 4340 VAR steel appears to be rather small. Indeed, in constant strain rate tests with the Kolsky bar, the flow stress level appears to be not more than 15% higher than in tests at a strain rate of 6×10^{-4} s^{-1}. This appears to be true for all three heat treatments. An increment in strain rate results in an increase in the stress level as shown in Figure 2 for the case of the 600C temper. The corresponding increments in stress are greater in the 425C temper even though the strains involved are much smaller.

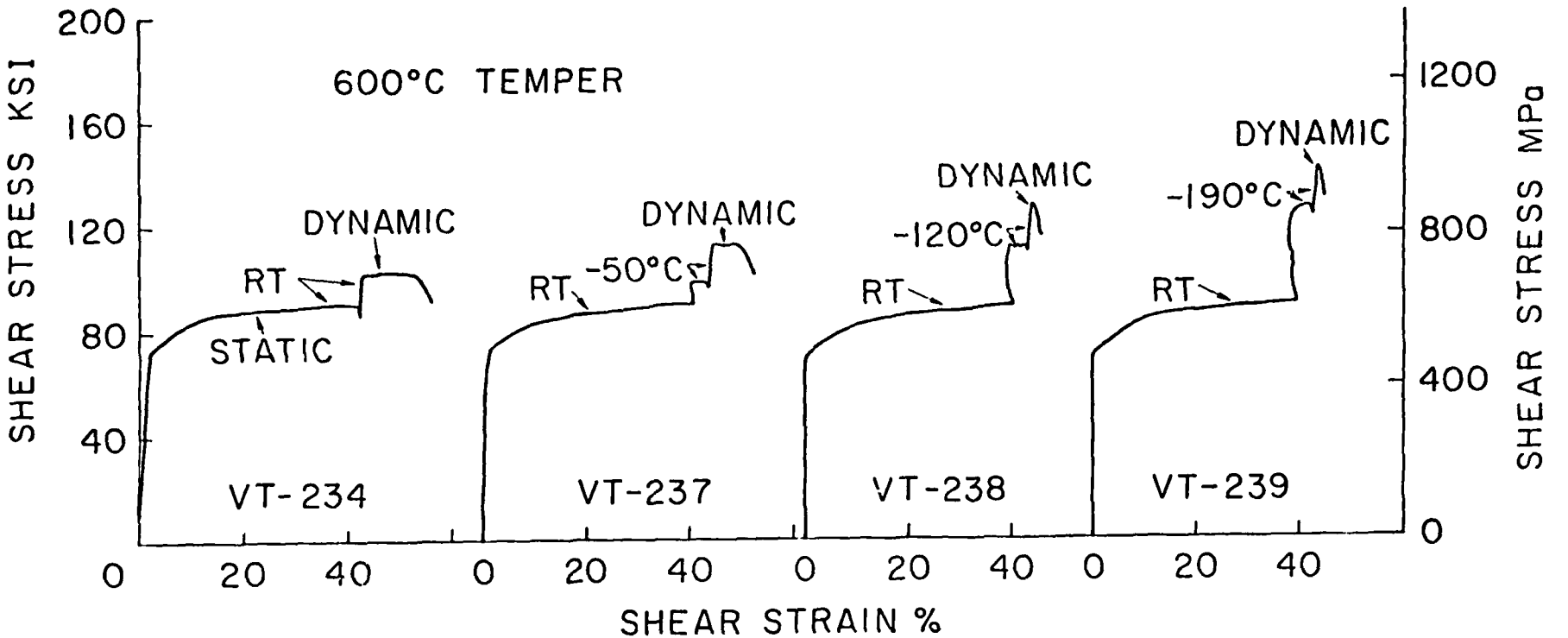

Fig. 2 Combined decremental temperature and incremental strain rate tests with specimens of 4340 VAR steel deformed in the torsional Kolsky bar. In this figure static deformation implies a strain rate of $6 \times 10^{-4} s^{-1}$ while dynamic implies $400\ s^{-1}$.

2.1.2 Strain-rate Sensitivity at Strain Rates of 10^5 s^{-1}

In order to study the strain-rate sensitivity of 4340 VAR steel at strain rates of the order of 10^5 s^{-1}, a series of pressure-shear plate impact experiments were conducted on thin specimens sandwiched between two hard steel plates. The pressure-shear experiment developed by LI (1982) under previous ARO support and used to study the plastic response of soft metals at strain rates of 10^5 s^{-1} was adapted to the measurement of the flow stress of 4340 VAR steel tempered at 600C. The principal modification of the technique was the introduction of exceptionally hard, as-quenched, tool steel as the material for the flyer and anvil plates. (See Fig. 3)

The results of these experiments are summarized in Fig. 4, taken from the Sc. M. thesis by KLOPP (1984). The flow stress shown by curves A thru E, neglecting the steeply rising parts of the curves for which the stress state in the specimen is not yet homogeneous, is approximately 30% greater than in static torsion tests and less than 15% greater than in torsional Kolsky bar experiments. Although there is appreciable scatter in the experimental results, it is evident that the flow stress tends to increase with increasing strain rate over the range of strain rates covered in the pressure-shear experiments; furthermore, the rate of increase appears to be comparable to the logarithmic increase with strain rate that is observed at lower strain rates. This lack of a transition in strain rate sensitivity at the high strain rates is consistent with the flow stress being far below the value required for plastic flow at 0^o K (from data of TANIMURA and DUFFY (1984) the latter value is extrapolated to be 900 MPa). Thus, the flow stress in the pressure-shear experiments appears to be in a regime where thermal activation of dislocations past obstacles is the dominant rate controlling mechanism. Variation of the skew angle and the velocity of impact revealed no measurable dependence of the flow stress on the hydrostatic pressure.

2.1.3 The Rate Tangent Modulus Method

A new numerical time integration method for use in finite element analyses of rate dependent solids was developed by PEIRCE, SHIH and NEEDLEMAN (1984). The method is explicit (no iterations are required) and convenient in that, unlike for other forward gradient type methods, no explicit matrix inversion is required. The method is, in essence, a generalization of the

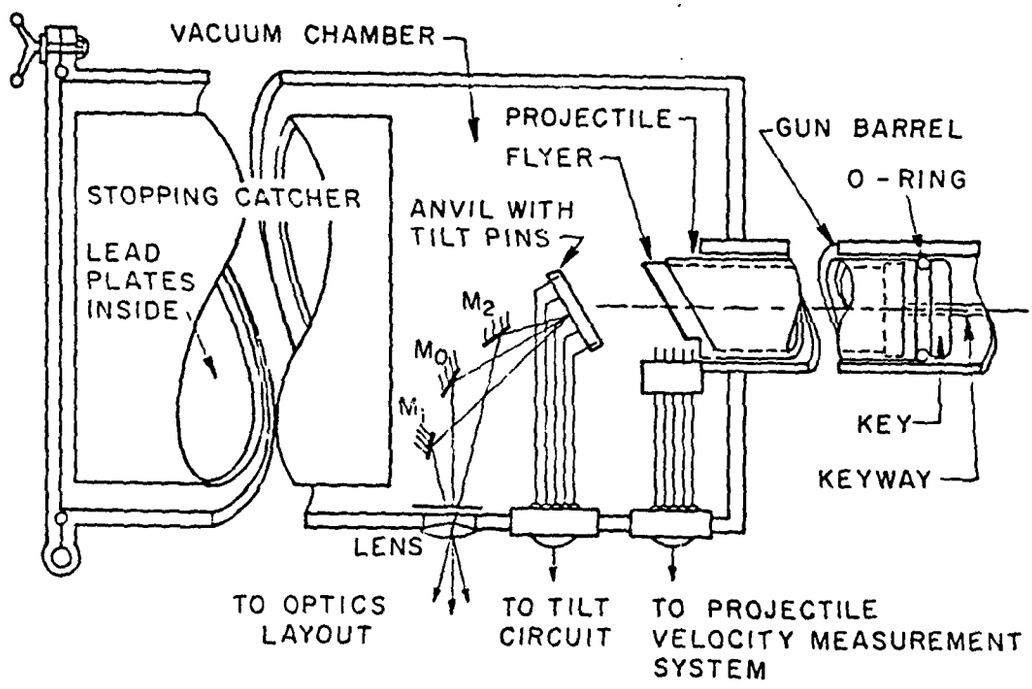

Fig. 3 Schematic of the pressure-shear plate impact experiment.

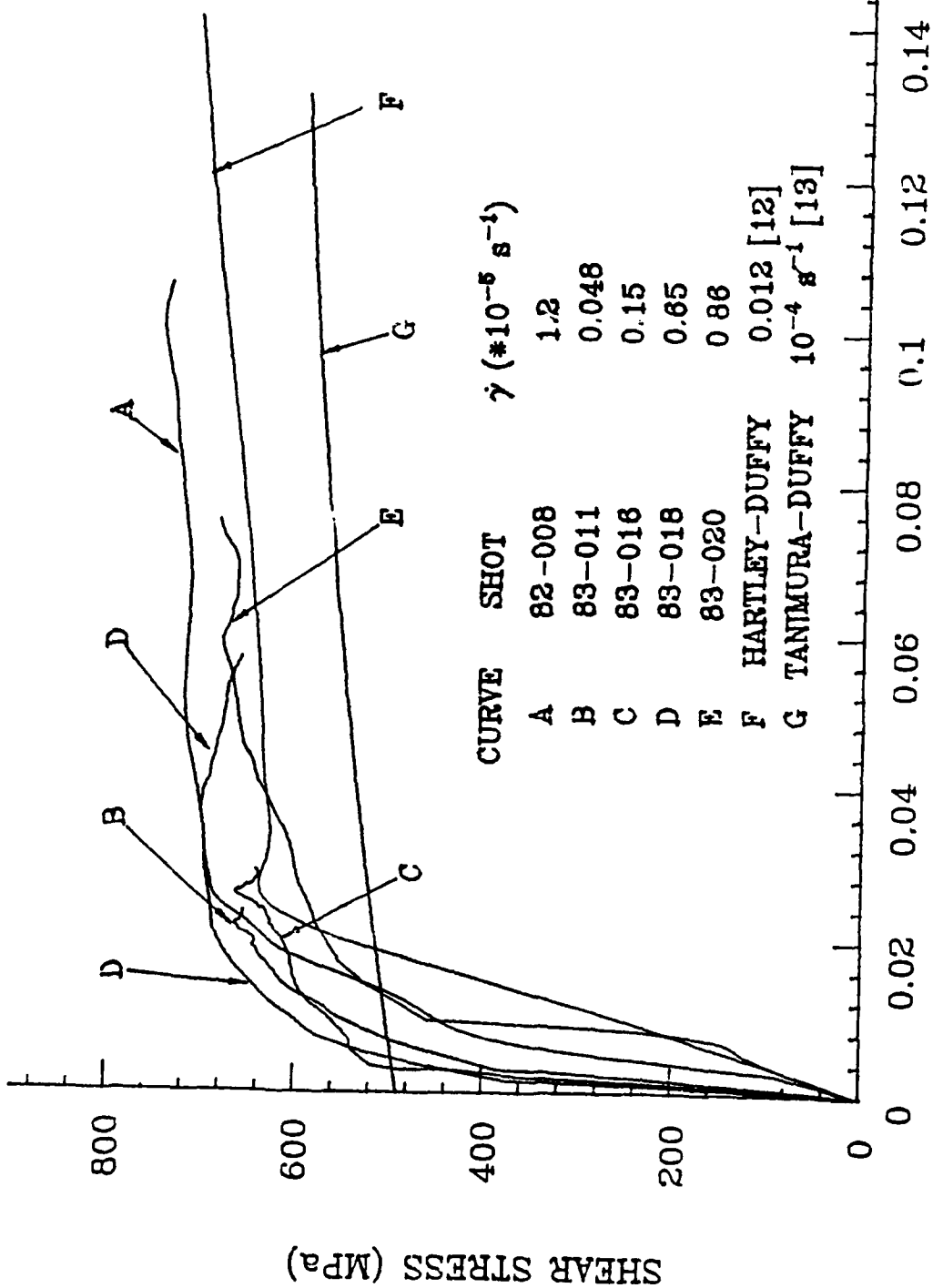

Fig. 4 Summary of the dynamic stress-strain curves obtained in pressure-shear impact of 4340 VAR steel, 600C temper. Stress-strain curves for quasi-static loading and for loading in the torsional Kolsky bar are included for comparison.

well known tangent modulus method for rate independent solids to allow for rate dependent material response. The method possesses several advantages over alternative approaches. In typical cases step sizes can be employed which are up to an order of magnitude greater than can be used with the simple Euler method. The method is stable even in the limit of nearly rate independent material behavior where traditional methods most frequently fail. However, it is important to note that the numerical stability of the method does not artificially mask physical instabilities. This is important since it means the method is suitable for analyzing problems of flow localization and failure. Indeed, the method has been succesfully employed in analyzing localized and non-uniform deformation modes including shear band initiation and propagation by PEIRCE, ASARO and NEEDLEMAN (1984)^{R}. Another attractive feature of the method is that governing finite element equations are readily derived for complex, microstructurally based constitutive relations. Application to a dilatant and pressure sensitive viscoplastic material model was discussed by PEIRCE, SHIH and NEEDLEMAN (1984) and the shear band study of PEIRCE, ASARO and NEEDLEMAN (1984)^{R} was carried out for rate dependent single crystals.

2.2 Shear Bands

2.2.1 Shear Band Experiments: Temperature Measurements

The thin-walled specimen used in the dynamic plasticity tests with the torsional Kolsky bar appears to be ideal for experiments on the formation of shear bands. The technique has been described in previous publications, which include descriptions of our early attempts to measure the temperature (DUFFY (1984)^{R}). Shear bands are detected by observations of the metal surface after testing to determine the uniformity of the strain distribution in the specimen. These observations are made by scribing a fine line on the specimen's surface and observing its inclination after deformation. (See Fig. 5). This provides a direct measure of the final shear-strain distribution.

An added convenience of the torsional Kolsky bar is that the maximum strain imposed can be set, independent of the strain rate. For some steels, this has permitted us to stop the deformation process just after the formation of microcracks within the shear band but before the crack runs around the entire circumference of the specimen.

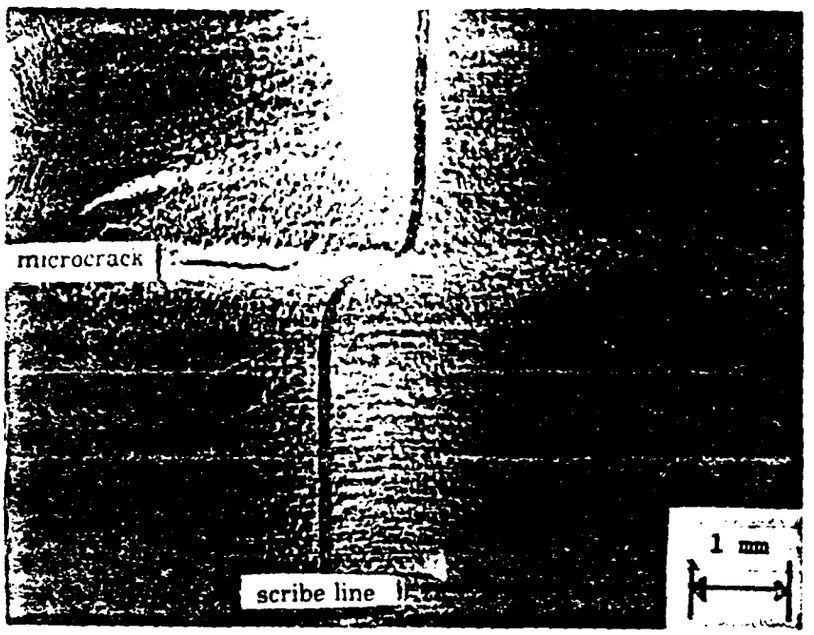

Fig. 5 Shear Band in 1018 CRS

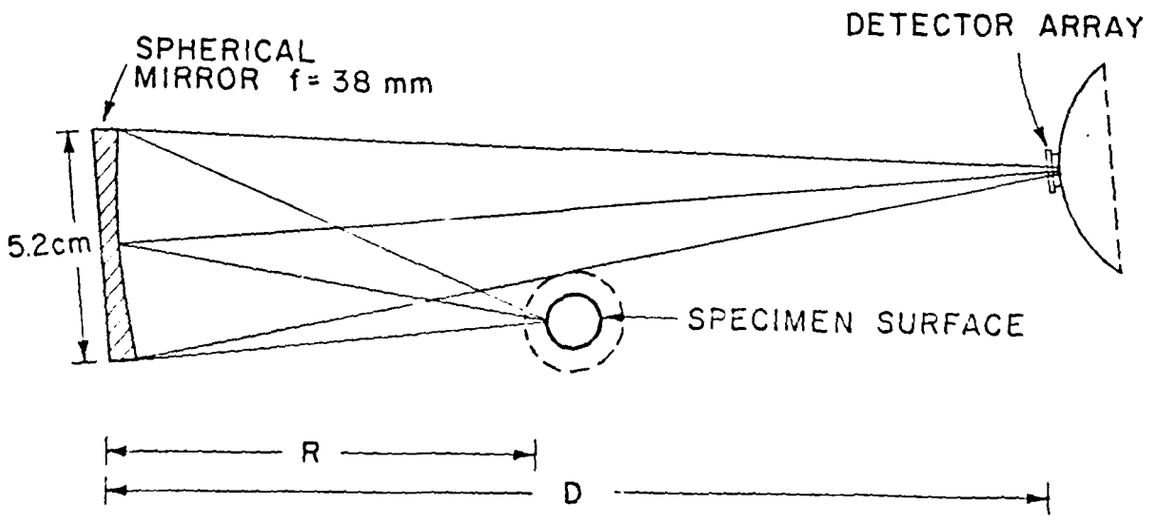

Fig. 6 Schematic diagram (not to scale) of infra-red Temperature Detector System with Adjustable Magnification capabilities (for 20 micron spot size on the specimen: R = 4cm and D = 80cm)

Estimates of the temperature rise in the shear band are made by measuring the infra-red radiation emanating from the specimen's surface. There are two problems in attempting any temperature measurement within the shear band. The first is the rapidity of the event. This difficulty is overcome in our experiments by measuring the surface radiation with indium-antimonide detectors that have a response time of about 100 nanoseconds. The second problem is the narrowness of the shear band in some steels; for example, in 4340 VAR steel a deformed band has a width of about 20 microns while the transformed band has a width of 5 to 20 microns. One additional difficulty, which occurs particularly with 4340 steel in the 200C temper, is that the specimen may fracture immediately after the shear band starts to form.

At present we are measuring the infra-red radiation by using a spherical gold-plated mirror to focus radiation from ten neighboring points on the specimen onto a series of ten indium antimonide detectors (HARTLEY and DUFFY (1984)). (See Figure 6) The output of the detectors is large enough that it is easily separated from the background radiation. The specimen spot size per element can be varied by varying the distances between the mirror and the specimen and the mirror and the detector array. We are currently using a specimen spot size of 20 microns, which is adequate for shear band measurements in cold-rolled steel in which the shear bands have a width of 200 microns or more. However, further refinement of the techniques is needed for accurate measurement of temperature in the narrow shear bands that occur in 4340 VAR steel.

We have attempted temperature measurements of shear bands in four steels: 1018 cold-rolled (CRS), 1020 hot-rolled (HRS), 4340 VAR, and 1215 steel with MnS inclusions. In the CRS a shear band invariably forms whenever the strain rate exceeds about 200 s^{-1}. For most of our tests the strain rate was about 1000 to 1200 s^{-1} and the shear band began forming at a strain of about 15%. The maximum observed temperature increase ranged from 206C to 440C in different tests, Figures 7 and 8. In view of the large width of the shear bands in CRS, these values are believed to represent quite accurately the temperature rise in the shear bands. The strain at fracture, averaged over the 0.25 cm specimen gage length including the width of the shear band, varied from 45% to 50%.

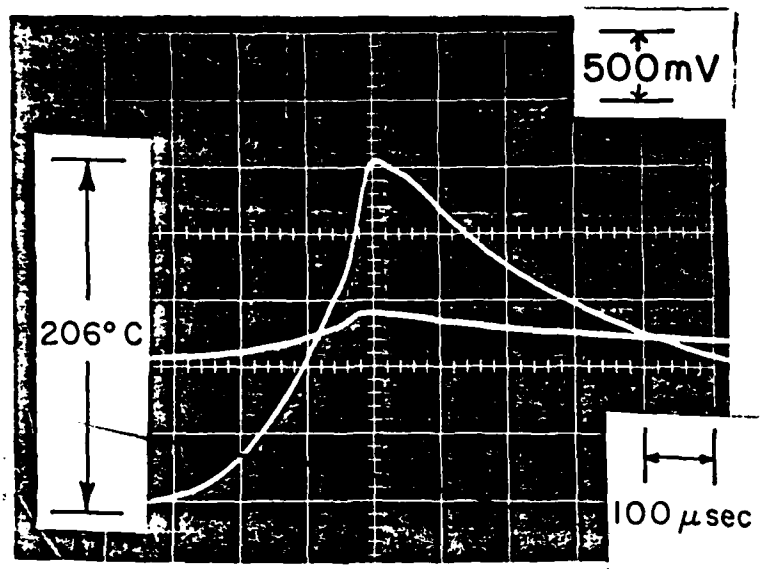

Fig. 7 Oscillograph showing output of two adjacent detector elements (CRS; spot size 0.25 mm)

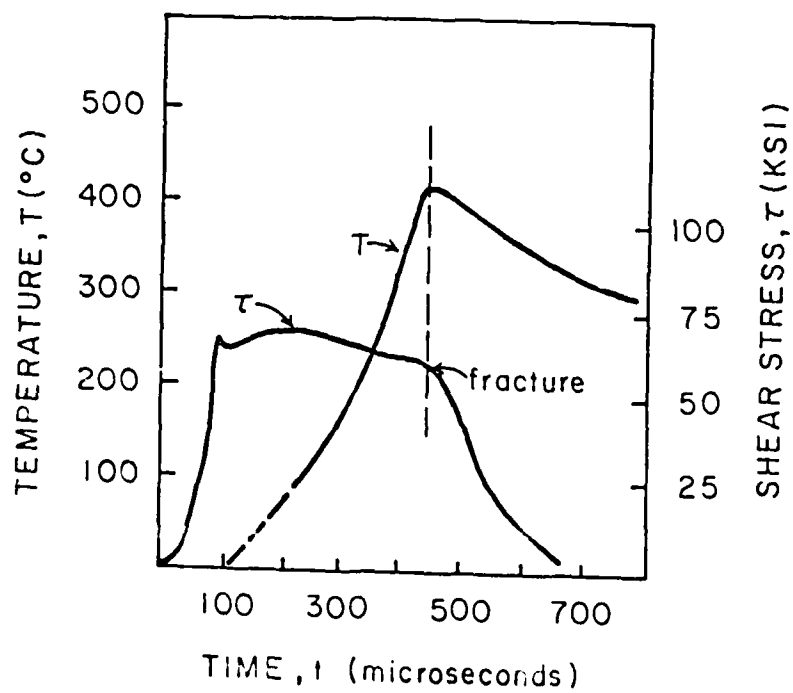

Fig. 8 Temperature and stress during Formation of Shear Band in CRS.

Shear bands in HRS do not occur as readily as they do in CRS. The tests on the 1020 HRS steel were prompted by the numerical study of Clifton and Shawki, based on experimental data, which suggested that shear bands may form in hot-rolled steel at a very high critical strain. Using a long pulse length and strain rates of about 2500 sec^{-1}, it was possible to achieve strains of over one hundred percent and obtain the flow stress maximum that is characteristic of shear band formation. Metallurgical examination showed that fracture often was accompanied by highly localized shear strain, the band width being approximately the same as in 1018 CRS, namely 250 microns. Measurements of the emitted infrared radiation proved that high temperatures were reached within the band, with a maximum temperature of 455°C recorded in one test.

In 4340 VAR steel the formation of shear bands depends very much on the temper. For the 200C temper it appears that shear bands do not form before the specimen fractures. However, since the total strain at fracture is quite small it would be difficult to observe shear bands even if they were present. For the other two tempers, shear bands form in all tests at strain rates greater than approximately 400 s^{-1}. For the 425C temper the shear band forms at a strain that may lie between 10% and 15%, apparently independent of the test temperature between -190C and 20C. For the 600C temper, the strain at which shear bands form decreases with decreasing test temperature: the variation is from 17% strain at -190C to 35% strain at 20C. Measured values of the temperature rise are about 425C. However, these values are for specimens in which the transformed band was only about half as wide as the diameter of the spot on which the infra-red detector is focussed, so that the peak temperature is undoubtedly greater. Clearly further work is required to improve this measurement.

The emphasis of our current work has been on refining our temperature measurement techniques to obtain a smaller spot size. For experiments on 4340 VAR steel this refinement is necessary to determine the temperature of a transformed band which is only 5-10 microns wide. The infrared microscope purchased from Barnes Engineering has been received and is being calibrated and tested in preparation for use in the shear band test. In addition, revisions to our present indium-antimonide detector/mirror system may allow temperature measurements over smaller spot sizes than 20 microns.

2.2.2 Analysis of Thermoplastic Instability in Simple Shear

As a means for gaining insight into the main features of thermoplastic instability we analyzed the case of simple shear of a material modeled as elastic, viscoplastic with thermal softening and heat conduction. A homogeneous shearing deformation was regarded as perturbed by either a geometric defect or by an initial nonuniformity of the stress and temperature. Explicit stability criteria were obtained for the elementary case of quasi-static, adiabatic, simple shear with stress-controlled boundaries (MOLINARI and CLIFTON (1983)). Strain hardening, strain-rate sensitivity, and thermal softening parameters determine the stability of homogeneous deformations for this elementary case. The general dynamic case, with heat conduction, was investigated by examining stability conditions for the linear perturbation problem with time-varying coefficients and by obtaining numerical solutions of the full nonlinear equations (SHAWKI, CLIFTON AND MAJDA (1983)). Three types of viscoplastic constitutive equations were considered. Velocity boundary conditions were emphasized, although stress boundary conditions were also examined. Numerical results were compared with the results of dynamic torsion experiments.

From these analyses we can conclude that strain rate sensitivity plays an important role in determining the rate at which an instability develops. For strong strain rate sensitivity, such as the linear dependence of shear stress on strain rate that is characteristic of Newtonian fluids, the rate of growth of inhomogeneous deformations is so slow that these deformations would not be characterized as forming shear bands. This lack of shear band development results even when there is essentially no strain hardening. In fact, shear bands are slow to form even in the case of weak strain softening. In contrast, for the case of weak strain rate sensitivity, such as the logarithmic or weak power law dependence of flow stress on strain rate that is characteristic of structural alloys, shear bands tend to form quickly once the slope of the stress-strain curve becomes negative due to strain hardening being overcome by thermal softening. For the case of a geometrical defect corresponding to a rectangular groove, significant localization in the groove occurs not when the slope of the local stress-strain curve first becomes negative in the groove, but after the slope of the local stress-strain curve becomes negative at positions distant from the groove. A heuristic interpretation of the phenomenology of shear band development due to

thermoplastic instability has been given for the idealized case in which elasticity and heat condition are neglected. In this case, which is a good approximation in such dynamic experiments as Kolsky bar experiments, short wavelength disturbances are predicted to grow faster than long wavelength disturbances (CLIFTON, DUFFY, HARTLEY and SHAWKI (1984)). Initially the former disturbances grow exponentially with increasing strain beyond the strain at which the slope of the stress-strain curve becomes negative. Weak strain rate sensitivity, weak strain hardening, and strong thermal softening increase the rate of growth of these short wavelength disturbances that tend to form shear bands.

Insight into such instabilities has been obtained by neglecting heat conduction and elasticity and considering the qualitative features of an ordinary differential equation for the plastic strain rate. The coefficients of this equation depend on unknown stress histories; however, using only the qualitative features of stress histories that are commonly obtained in complete numerical solutions, one obtains significant understanding of critical steps in the development of the unstable response. In particular, the qualitative analysis provides a means for differentiating between shear bands in which the width of the bands remain comparable to the width of the inhomogeneity and those in which the width becomes much narrower than the initial inhomogeneity SHAWKI (1985). The latter type of instability is a very strong instability that is believed to correspond to the formation of very narrow shear bands in high strength steels at high strain rates.

2.2.3 Analysis of Deformation Trapping

The results of a theoretical study of the phenomenon of deformation trapping due to thermoplastic instability in one-dimensional wave propagation have been reported by WU and FREUND (1984). In this study, one-dimensional shear wave propagation in a half space of a non-linear material was considered. The surface of the half space was subjected to a time dependent but spatially uniform tangential velocity. The half space material was assumed to exhibit strain hardening, thermal softening and strain rate sensitivity of the flow stress. It was found that, for this process, a well-defined band of intense shear deformation can develop adjacent to the loaded surface, even though the material has no imperfections or other natural length scale.

First, a simple model based on linear rate sensitivity was examined to illustrate qualitatively how the various competing effects in the process could result in a band. Then, results of numerical calculations for materials with linear or logarithmic rate sensitivity and for processes which were adiabatic or with heat conduction were reported. The influence of heat conduction was found to be minimal for realistic loading rates, and the results were assessed in terms of the limited experimental data available for the process.

2.2.4 Analysis of the Propagation of Shear Bands

A mechanism by which shear bands are formed in materials under high rates of deformation has been considered by WU, TOULIOS and FREUND (1984). It was assumed that the bands initiate due to strain concentrations at material or geometrical defects, and that they propagate in a crack-like fashion to become the bands observed in laboratory specimens. As a model, the two-dimensional antiplane shear deformation of a large block of incompressible, hyperelastic material was considered. To simulate the phenomenon of thermal softening due to adiabatic heating, a material model was selected which showed a local maximum in the dependence of shear stress on shear strain. The block was presumed to contain a small region in which the stiffness was less than in the remainder of the otherwise homogeneous material. Initially, the block was assumed to have no strain and a spatially uniform strain rate. At points remote from the defect, loads were applied to produce a constant average strain rate for later times. A complete numerical solution of the problem was obtained by means of a finite element discretization of the body and by use of a finite difference method to integrate the differential equations for the evolution of the nodal variables in the finite elements. It was found that the strain in the block remains more or less uniform until the time at which the condition for instability is met in the defect. Strain is then rapidly concentrated at the edge of the defect, and a shear band grows at a very high speed from the defect into the remainder of the block. It is important to note that this happened for average strain levels which were subtantially below the critical strain level for the material outside of the defect. The speed of propagation of the edge of the band was found to be nearly independent of the level of background strain, and to compare very well with the speed predicted by linearizing the governing equations around the critical state of the material.

In a follow-up study, a block which contained several neighboring regions of imperfection was considered in order to study interactions which could occur during the formation of bands (WU (1984)). Through numerical analysis, three different mechanisms of interaction were identified, with the particular type depending on the relative positions and strengths of the defects. The three types of interaction may be identified briefly as follows: (i) a primary band is arrested by a nearby defect, but a secondary band is initiated from the nearby defect, (ii) a primary band propagates beyond a nearby defect and supresses the formation of a band from the nearby defect, and (iii) the defects produce bands independently and without interaction.

A supporting study on the wavefront induced in a homogeneously shearing solid by a localized material imperfection has been completed by TOULIOS (1984). In this study, a body of incompressible, hyperelastic material was assumed to be undergoing rapid homogeneous shear strain. The material model was such that strong ellipticity of material response fails at a strain level corresponding to the local maximum of the shear stress-strain relation. A point imperfection was suddenly introduced in the material. It was shown that the rays of the hyperbolic system of equations representing the superimposed wave motion tend to curve away from the direction of the ongoing background strain; the wavefront patterns provide a clear illustration of the directional nature of the growth of the superimposed deformation. The results extend the wave trapping idea to two-dimensional wave fields.

The plane strain, quasi-static deformation of a softening visco-plastic solid with an initial weak spot has been analyzed. The specific boundary problem treated is a rectangular block subject to plane strain tension, with the sides of the block constrained to remain straight to rule out diffuse necking. This lateral boundary condition corresponds to assuming periodicity in the transverse direction. The material is taken to be a visco-plastic Mises solid with strain rate hardening, but with strain softening after a plastic strain of 0.1. The material is power law strain rate hardening with an exponent of 0.002. A finite element solution has been carried out for a block with one soft element; when the material properties are uniform, the solution to the boundary value problem analyzed is a state of homogeneous plane strain tension. In order to resolve intense shearing in a narrow band, we use a

finite element method developed for shear band propagation in rate independent solids TVERGAARD, NEEDLEMAN and LO, (1981)[R] and extended to visco-plastic solids PEIRCE, ASARO and NEEDLEMAN (1983)[R]). Strain contours at an extension of 0.20 show shear bands developing at 45° from the tensile axis and strong strain concentrations at intersections of shear bands originating at neighboring inhomogeneities. Our finite element method encounters no special difficulty in treating strain softening and shear band propagation. We plan to couple this program with our previously developed heat conduction program so that the modeling of softening with increased strain can be related directly to thermal softening.

2.3 Fracture

2.3.1 Correlations of Microstructure with Plasticity and Fracture Initiation Toughness in Plain Carbon Steels

As a means of understanding the effects of microstructure and heat treatment on fracture initiation in plain carbon steels an experimental study has been carried out of dynamic and quasi-static plane strain fracture toughness in an AISI 1020 steel. The steel was heat treated to obtain a range of microstructures. Two loading rates were used to initiate dynamic fracture at a stress intensity rate of $\dot{K}_I = 2 \times 10^6$ MPa $m^{\frac{1}{2}}$ s^{-1} and quasi-static fracture at a rate of $\dot{K}_I = 1.0$ MPa $m^{\frac{1}{2}}$ s^{-1}. Heat treatments were designed to vary both ferrite and prior austenite grain size over an appreciable range but the microstructures chosen for study all had very similar uniaxial tensile properties. In addition, for the purpose of analysis of the fracture tests and to allow for micromodelling of the fracture initiation mechanisms, a series of quasi-static and high rate plasticity tests were conducted. The fracture tests and the plasticity tests were conducted over the temperature range -150C to 100C; our plans call for an extension of the testing temperatures to 150C in the near future. This temperature range includes both "lower shelf" cleavage fracture, and "upper shelf" fibrous fracture, and thus allows for a thorough study of the ductile-brittle transition.

The dynamic fracture initiation tests were conducted on stress wave loaded V-notched circular rods using the methods originally developed by COSTIN, DUFFY and FREUND (1977)[R] and further developed by WILSON, HAWLEY and DUFFY (1980)[R] and by COUQUE, DUFFY and ASARO (1984) in the present study. The experimental configuration used in the present work is shown in Fig. 9. The notched section of the specimen is prefatigued by a rotating beam apparatus of set displacement so that the fatigue annulus produced is circular. In these tests, the depth of the fatigued precrack was made so the ratio of ligament diameter to bar diameter was 0.3. The torsion tests were conducted in the modified split Kolsky bar developed at Brown by DUFFY, CAMPBELL and HAWLEY (1971)[R]. Three different microstructures were chosen for investigation. They were formed using simple normalization type heat treatments where the two main variables were austenitizing temperature (to control prior austenite grain size) and cooling rate (to control ferrite grain size).

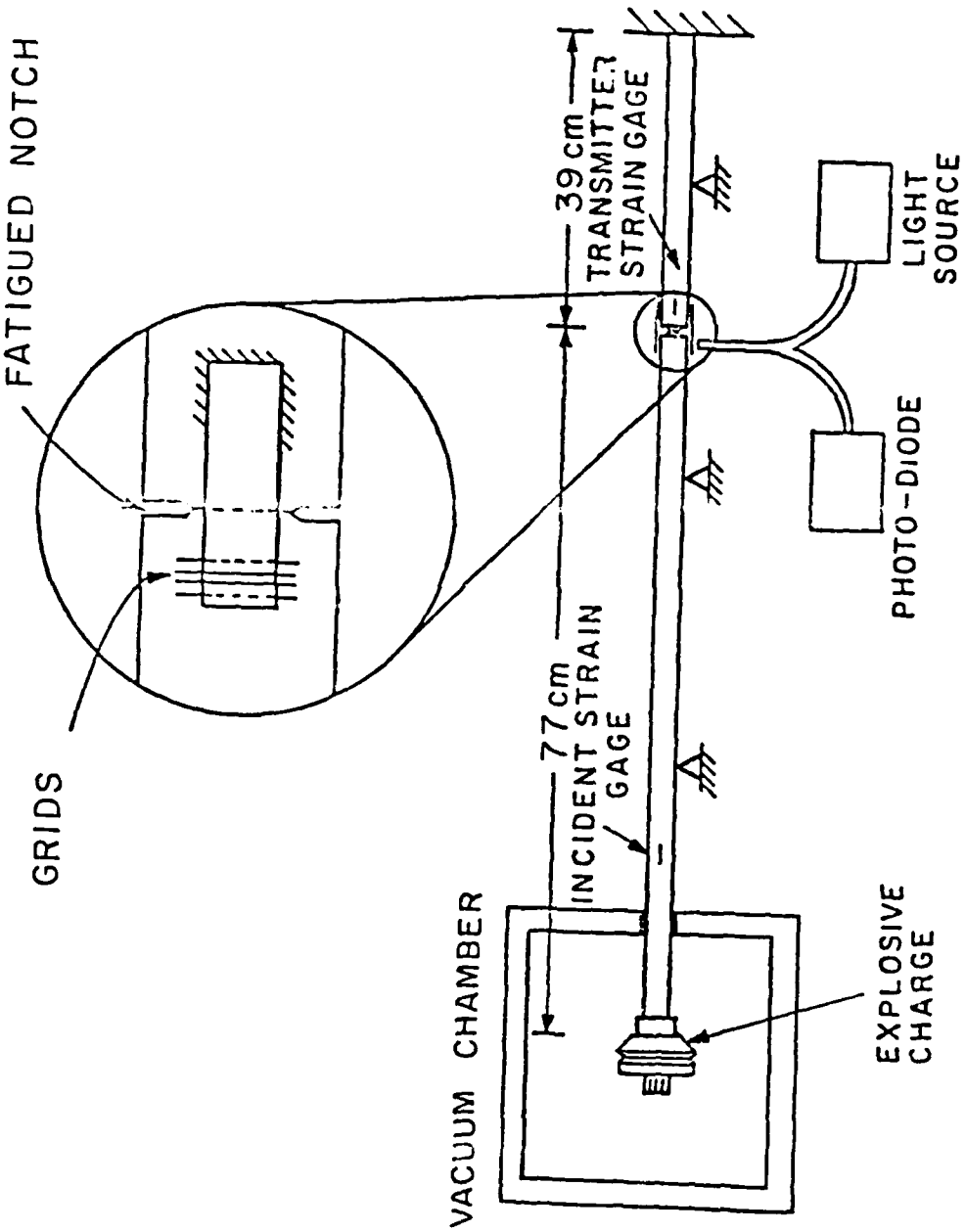

Fig. 9 Schematic of Dynamic Fracture Initiation Experiment.

Figure 10 shows a comparison of the shear stress-shear strain curves obtained quasi-statically at the three temperatures -60C, 23C and 60C for the microstructure T1 characterized by the finest austenite and ferrite grain sizes, and the microstructure T7 characterized by the largest austenite and ferrite grain sizes. At temperatures greater than 23C the flow stress curves for these two microstructures are very similar, with the finer microstructure displaying a slightly greater strength. At lower temperatures there is the interesting trend for the coarser microstructure to display a larger flow stress. In part this may be due to the larger volume fraction of pearlite formed during the slow cooling of the coarse microstructure. A more complete set of data for shear stress-shear strain curves is given by COUQUE, DUFFY and ASARO (1984). In general, these data show a strong temperature sensitivity of flow stress and a trend for the finer microstructure to display slightly higher flow stresses at temperatures larger than 23C. In all cases the microstructures studied were quite ductile.

Figure 11 shows results for the dynamic and quasi-static plane strain fracture toughness over the temperature range -150C to 100C. The proportions of cleavage and fibrous fracture have been measured and are reported by COUQUE, DUFFY and ASARO (1984); on Figure 11 the fracture mode is indicated qualitatively as follows: "C" designates 100 percent cleavage, "F" 100 percent fibrous, and "CF" mixed cleavage-fibrous. When fractures occur by cleavage the dynamic fracture toughness values K_{ID}, are observed to be lower than the quasi-static, K_{IC}, values. However, at temperatures at which fractures are fully fibrous the dynamic toughness is significantly larger than the quasi-static toughness. It appears that in large part the effect can be attributed to the fact that the fibrous fractures, whether static or dynamic, require comparable, and large, plastic strains. Since these strains occur at higher stresses in the dynamically loaded specimen, the toughness tends to be larger. The quasi-static fracture toughness, on the other hand, shows a very interesting phenomenology in the temperature range between -60C and 60C, i.e., in the middle of the ductile-brittle transition range. At the temperatures 23C and 60C the fracture toughness for the coarse microstructure T7 is larger than that of the finest microstructure, T1. This trend is not displayed by other measures of toughness such as Charpy impact energy and appears to be linked to the size scale, and spacings, of the microstrutural features that

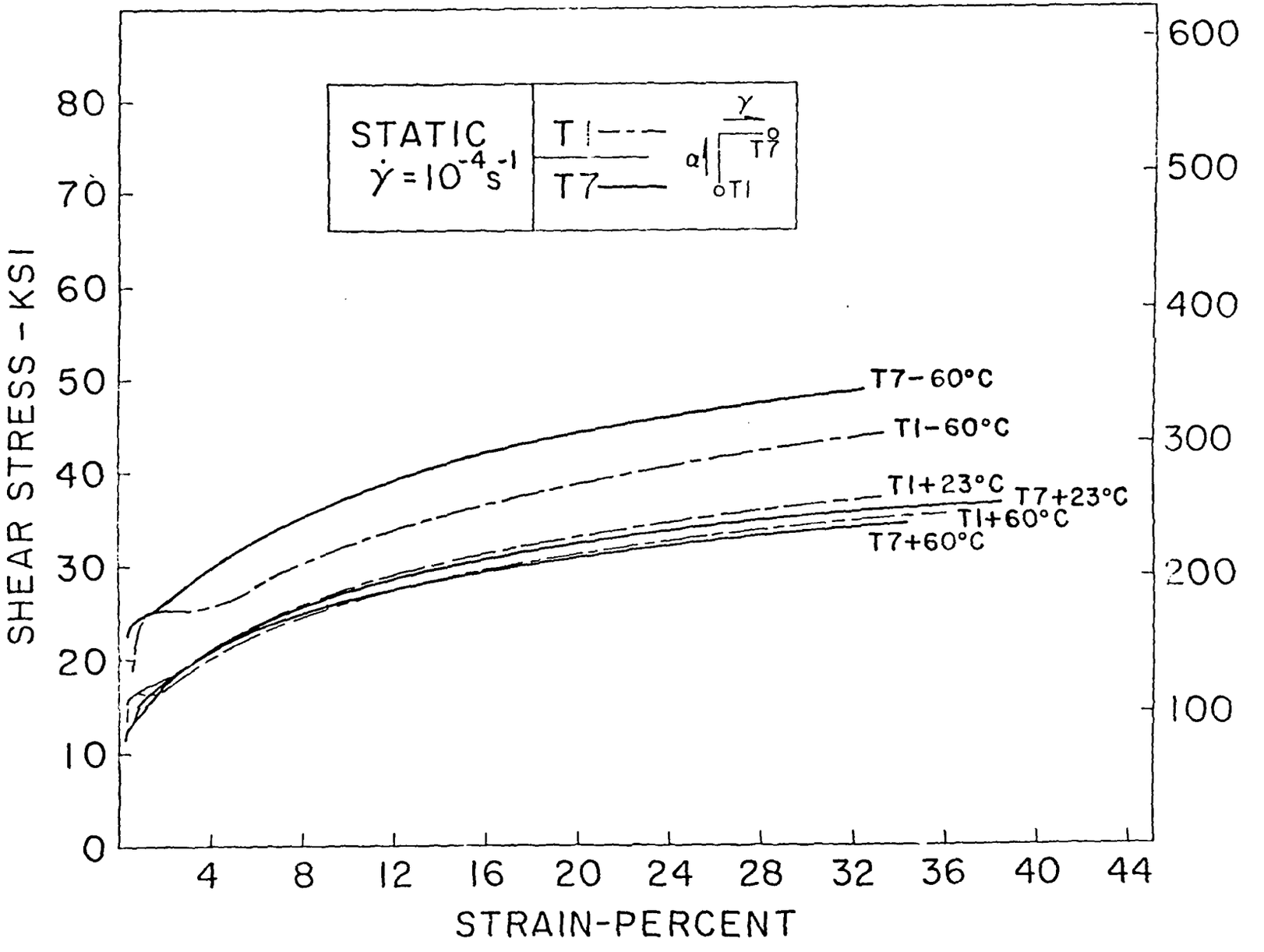

Fig. 10 Quasi-static Stress Strain Curves in Torsion for the Coarsest and Finest Microstructures of the AISI 1020 Steel, Over the Temperature Range of the Ductile/Brittle Transition.

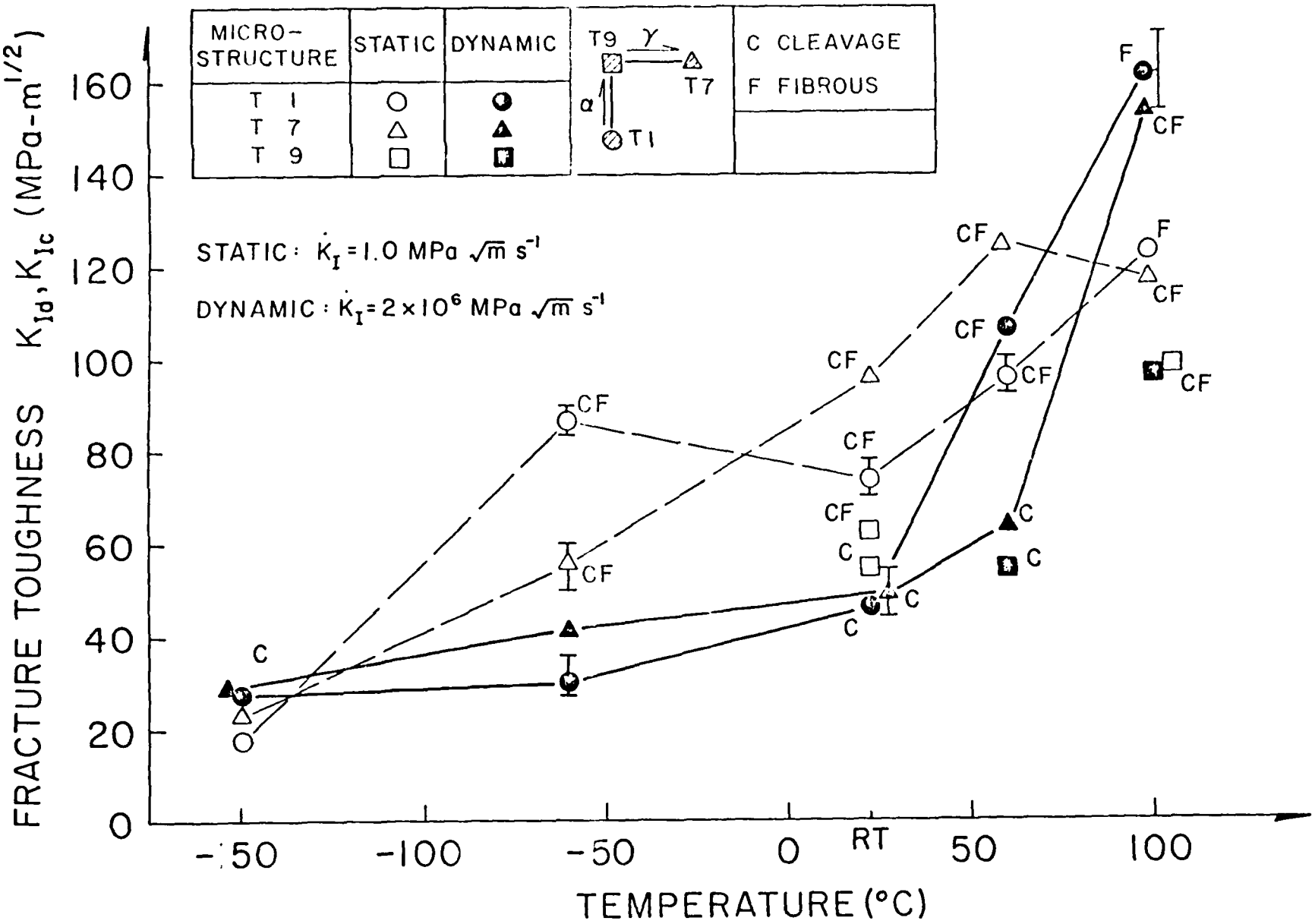

Fig. 11 Quasi-static and Dynamic Fracture Toughness of AISI 1020 Steel with Different Microstructures.

initiate fracture in the stress-strain fields of a sharp crack tip. This finding has led to a detailed study of the fracture initiation phenomenon in the ductile fracture regime in an effort to distinguish unambiguously the instant of fracture initiation. As a part of this study we are now calibrating the electrical resistance technique for detecting crack growth by wedging open the notch when crack growth is indicated. This is followed by unloading, sectioning, polishing and microscopic examination to determine the actual extent of crack growth. In addition simultaneous compliance tests are being conducted.

Quasi-static tests of specimens of a third type having the finer prior austenite and the larger ferrite grain sizes have been completed over the temperature range of -150°C to +60°C with some tests at 100°C.

Considerable effort has been expended in improving our means for detecting fracture initiation in the case of ductile fractures. The method we have been using involves monitoring changes in electrical resistance across the fracture zone. Recently, this resistance measurement has been improved by reducing considerably the electrical noise and drift associated with the apparatus thus resulting in a significant reduction in variation of results.

2.3.2 Modeling of Ductile Fracture

In order to study the influence of stress state on ductile failure in high strength steels, HANCOCK and MACKENZIE (1976)[R] and HANCOCK and BROWN (1983)[R] carried out tests on axisymmetric and plane strain blunt and sharply notched tensile specimens. Their comparison of test results with solutions based on classical plasticity theory (J2-flow theory) indicated that the onset of ductile rupture is represented approximately by a single failure locus in a plot of stress triaxiality versus accumulated plastic strain at the failure site.

When microscopic voids nucleate and grow in a ductile metal the average macroscopic effects are a plastic dilatancy, a pressure sensitivity of plastic flow and, possibly, a non-associated flow rule. A model of a porous plastic solid incorporating these macroscopic effects is due to GURSON (1975)[R]. This constitutive model has been used by NEEDLEMAN and TVERGAARD (1984) to analyze

the influence of stress state on ductile fracture. Calculations were carried out for plane strain and axisymmetric blunt and sharply notched specimens. The specimen geometries were taken to be those used in the experiments of HANCOCK and MACKENZIE (1976)[R] and HANCOCK and BROWN (1983)[R]. The computations make it possible to study the influence on void growth of the relatively high strains at the surface and the high triaxiality at the center.

The computed plots of stress triaxiality versus plastic strain show path dependence. However, for reasonably small deviations from a proportional stress history a single failure locus is found to hold approximately. Interestingly, there is a certain systematic trend in the deviation from a history independent failure locus. Failure initiation in the plane strain, blunt-notch specimens occurs with lower triaxiality and at a smaller value of effective strain than for the corresponding axisymmetric, blunt-notch specimens. This behavior of the plane strain blunt-notch specimens is an effect of shear localization. A smaller fracture strain is expected in cases where failure involves localization and, in general, plane strain states are more susceptible to localization than axisymmetric deformation states. Previous studies of localization in porous plastic solids, have found that localization in plane strain typically occurs at relatively small void volume fractions (NEEDLEMAN and RICE, 1978; TVERGAARD, 1981; SAJE, PAN and NEEDLEMAN, 1982)[R]. However, it is important to note that the critical strains given by such analyses refer to the strain level outside a shear band, whereas the actual failure point may be inside a band. Full calculations of shear band development have shown that the localized strains required for coalescence inside a band are large (e.g. TVERGAARD, 1982)[R]. Thus, for the onset of failure as defined here, localization can precede failure and lead to a strong deviation from proportional loading at the eventual failure site.

Another important issue concerns the extent to which an analysis using the classical, plastically incompressible, Mises flow rule gives stress and strain values representative of local conditions in a voided solid. Void nucleation and growth leads to a lowering of local stress levels due to the softening that develops with increasing porosity. An additional important effect we find is the loss in triaxiality in plane strain associated with increasing porosity. In nonuniform deformation fields such as occur in the

notched bar analyses, this effect can take place gradually over the deformation history and leads to a significant redistribution of stresses. It should also be emphasized that local stress and strain values obtained from an analysis based on the Mises flow rule cannot reflect the effects of plastic flow localization. Especially for plane strain specimens with blunt notches, stress triaxiality levels inferred from calculations for an incompressible Mises solid may not be representative of local conditions in a voided solid at failure initiation. On the other hand, for more sharply notched plane strain specimens and for the axisymmetric specimens, an analysis based on the Mises flow rule would predict triaxiality levels at failure initiation that differ little from the ones we obtain. Although, as mentioned above, once failure initiates the differences do become substantial.

The constitutive relation we employ in the calculations is a modified version of the one originally proposed by GURSON (1975)[R] and gives material failure, i.e. a complete loss of stress carrying capacity, at achievable strain levels. It is important to emphasize that in our calculations the development of failure, i.e. crack initiation and growth, occurs as a natural consequence of severe deformation and does not involve any a priori failure criterion. In a previous study of failure in axisymmetric tension, TVERGAARD and NEEDLEMAN (1984), the crack in its initial stages of growth was confined to near the plane of minimum cross section by the constraint of the axisymmetric geometry. In this study, we carried out a calculation of the initial stages of crack growth in a plane strain blunt notched specimen. We find the computed crack growth to be straight ahead. In this case, it is not a geometric constraint, but rather the strong gradients associated with the sharp notch geometry that act to confine crack growth to the midsection plane. Several features of this failure process are noteworthy. First, failure does not initiate at the notch surface but slightly below. This is actually expected since the stress free condition on the notch surface lowers the surface stress levels. Once initiated, the failure region propagates both backward toward the notch and forward into the material. Each subsequent failed element is somewhat removed from the newly created free surface. The failed region remains along the row of elements nearest the midsection despite a clear tendency to shear banding.

Although a quantitative comparison with the experiments of HANCOCK and MACKENZIE (1976)[R] and HANCOCK and BROWN (1983)[R] is not made, the calculations do provide accurate qualitative descriptions of the observed failure process in notched specimens and of the observed effects of stress and deformation state.

2.3.3 Fracture at Ultra-High Loading Rates

In order to investigate dynamic fracture at loading rates that occur during impact loading of high strength structural elements we have developed a plate impact technique for studying fracture initiation at loading rates of the order of $K_I = 10^8$ MPa $m^{\frac{1}{2}}$ s^{-1}. The specimen consists of a circular disc with a mid-plane, prefatigued, edge crack that has propagated halfway across the diameter as shown in Figure 12 (CLIFTON AND RAVICHANDRAN (1983)). A compressive pulse propagates through the specimen, reflects from the rear surface, and subjects the crack plane to a step tensile pulse. According to linear elastic fracture mechanics the crack tip stress intensity factor K_I increases as a known factor multiplied by $t^{\frac{1}{2}}$ where t is the time after the arrival of the tensile step wave at the crack plane. The critical value of K_I for fracture initiation can therefore be obtained if the time at which crack propagation begins can be determined. This time of fracture initiation is to be obtained by monitoring the motion of the rear surface of the specimen with a laser interferometer and observing the time at which waves emanating from the crack tip at fracture initiation arrive at the rear surface.

Experiments have been conducted on 4340 VAR steel specimens tempered at 200C. Crack front positions before and after impact have been located accurately by means of focussed ultrasonic waves. For tensile pulse durations of 1.0 sec the crack advances from 0.6 - 1.9 mm for the range of impact velocities used. The feasibility of the experiment and the existence of sub-microsecond crack propagation at velocities of one-half the elastic shear wave speed or higher have been established. A remaining difficulty is the determination of the critical conditions for fracture initiation by relating the near tip stress field at fracture initiation to the measured motion of the rear surface. So far this motion has not agreed with predictions based on elastic wave theory -- even at times before crack propagation is expected. Scanning electron microscope observations reveal fully fibrous fracture

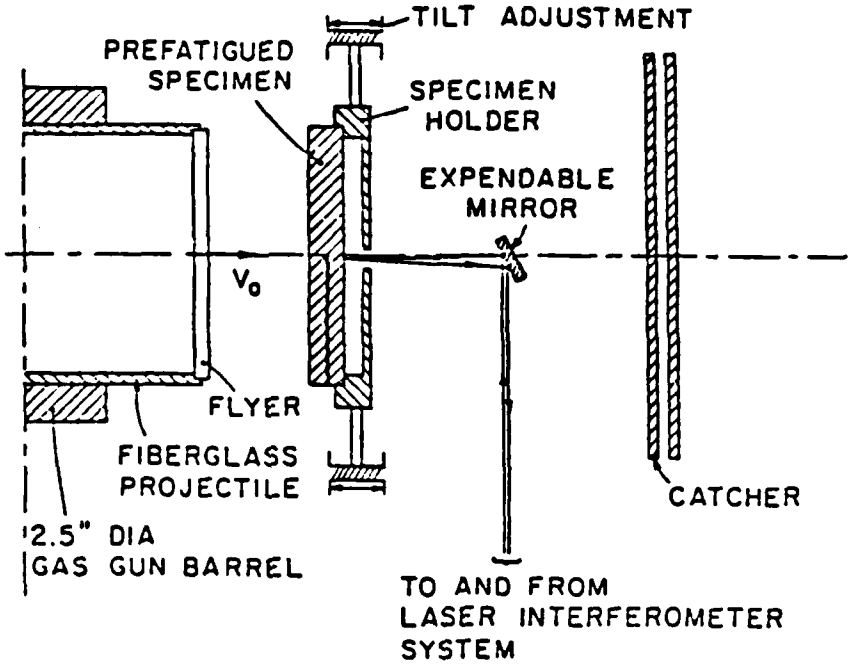

Figure 12 Schematic of Plate Impact Experiment for Dynamic Fracture at High Loading Rates.

surfaces at dynamic fracture initiation. Thus, it appears that crack tip plasticity may be responsible for the discrepancy between predicted and measured rear surface motions.

Plate impact fracture experiments on pre-cracked plates of 4340 VAR steel have been extended to low temperatures (-110°C) in an attempt to obtain fracture in a pure cleavage mode. Fracture surfaces observed by SEM show cleavage across grains but extensive plastic shearing and hole growth in the vicinity of grain boundaries. Fracture initiation, however, appears to occur by pure cleavage and the initial motion of the rear surface is more clearly in agreement with elastodynamics predictions. Propagation distances increase with decreasing temperature in accord with a decrease in fracture toughness at low temperatures.

3. PUBLICATIONS, REPORTS and THESES

CLIFTON, R. J. 1983 "Dynamic Plasticity" J.Appl.Mech. 50, 50th Anniversary Issue, pp. 941-952.

CLIFTON, R. J., GILAT, A. and LI, C. H. 1983 "Dynamic Plastic Response of Metals Under Pressure-Shear Impact," in Material Behavior under High Stress and Ultrahigh Loading Rates, edited by J. Mescall and V. Weiss, Plenum, pp. 1-19.

CLIFTON, R. J. 1983 "Pressure-Shear Impact and the Dynamic Plastic Response of Metals," Proceedings of the APS 1983 Topical Conference on Shock Waves in Condensed Matter, edited by J. R. Asay, G. K. Staub and R. A. Graham.

CLIFTON, R. J. and RAVICHANDRAN, G. 1983 "A Plate Impact Experiment for Studying Crack Initiation at Loading Rates $K_I \quad 10^8$ MPa $m^{\frac{1}{2}}$ s^{-1}", Proceedings of the NSF and ARO Workshop on Dynamic Fracture, Edited by W. G. Knauss, K. Ravi-Chandar, and A. J. Rosakis, pp. 36-46.

CLIFTON, R. J., DUFFY, J., HARTLEY, K. A. and SHAWKI, T. G. 1984 "On Critical Conditions for Shear Band Formation at High Strain Rates," Scripta Met. 18, pp. 443-448

COUQUE, H. 1984 "Effect of Prior Austenite and Ferrite Grain Size on Fracture Properties of a Plain Carbon Steel", Sc.M. Thesis, Division of Engineering, Brown University.

COUQUE, H., DUFFY, J. and ASARO, R. J. 1984 "Effects of Prior Austenite and Ferrite Grain Size on Fracture Properties of a Plain Carbon Steel", Technical Report, No. ARO DAAG29-81-K-0121/7, Division of Engineering, Brown University.

HARTLEY, K. A. and DUFFY, J. 1984 "Measurement of Temperature during the Formation of Shear Bands In AISI 1018 Cold-Rolled Steel" Technical Report, Division of Engineering, Brown University, in preparation.

KLOPP, R. W. 1984 "Pressure-Shear Deformation of 4340 Steel at Strain Rates of 10^5 s^{-1}," Sc. M. Thesis, Division of Engineering, Brown University.

KLOPP, R.W. and CLIFTON, R.J. 1984 "Pressure-Shear Plate Impact Testing", in Mechanical Testing, Vol. 8 9th ed., Metals Handbook, American Society of Metals (to appear).

LI, C. H. 1982 "A Pressure-Shear Experiment for Studying the Dynamic Plastic Response of Metals at Shear Strain Rates of 10^5 sec^{-1}," Ph.D. Thesis, Division of Engineering, Brown University.

MOLINARI, A. and CLIFTON, R. J. 1983 "Localisation de la deformation viscoplastique en cisaillement simple: resultats exacts en theorie non lineaire," C.R. Acad. Sci. Paris 296, pp. 1-4.

NEEDLEMAN, A. and TVERGAARD,V. 1984 An Analysis of Ductile Rupture in Notched Bars, J. Mechs. Phys. Solids, 32, p. 461.

PEIRCE, D., SHIH, C. F. and NEEDLEMAN, A. 1984 "A Tangent Modulus Method for Rate Dependent Solids", Comp. Struct. 18, p. 875.

RAVICHANDRAN, G. 1983 "A Plate Impact Experiment for Studying Crack Initiation at Loading Rates K_I 10^8 MPa $m^{\frac{1}{2}}$ s^{-1}," Sc. M. Thesis, Division of Engineering, Brown University.

SHAWKI, T. G. 1983 "Analysis of Shear Strain Localization in Thermal Visco-Plastic Materials," Sc. M. Thesis, Division of Engineering, Brown University.

SHAWKI, T. G., CLIFTON, R. J., and MAJDA, G. 1983 "Analysis of Shear Strain Localization in Thermal Visco-Plastic Materials," Technical Report No. ARO DAAG29-81-K-0121/3, Division of Engineering, Brown University.

TANIMURA, S. and DUFFY, J. 1984 "Strain Rate Effects and Temperature History Effects for Three Different Tempers of 4340 VAR Steel" Technical Report, No. ARO DAAG29-81-K-0121/4, Division of Engineering, Brown University, in preparation.

TOULIOS, M. 1984 "The Wavefront Induced in a Homogeneously Shearing Solid by a Localized Material Imperfection", Quarterly of Applied Mathematics, to appear.

WU, F. H. and FREUND, L. B. 1984 "Deformation Trapping Due to Thermoplastic Instability in One-dimensional Wave Propagation", Journal of the Mechanics and Physics of Solids 32, pp. 119-132.

WU, F. H., TOULIOS, M. and FREUND, L. B. 1984 "Initiation and Propagation of Shear Bands in Antiplane Shear Deformation", Technical Report No. ARO DAAG29-81-K-0121/6, Division of Engineering, Brown University.

WU, F.H. 1984 "A Study of Strain Localization in Solids Undergoing Rapid Shearing, Ph.D Thesis, Division of Engineering, Brown University.

4. REFERENCES

COSTIN, L. S., DUFFY, J. and FREUND, L. B. 1977 — ASTM STP 627, 301.

DUFFY, J. CAMPBELL, J. D. and HAWLEY, R. H. 1971 — J. Appl. Mech. 38, 83.

GURSON, A. L. 1975 — Plastic Flow and Fracture Behavior of Ductile Materials Incorporating Void Nucleation, Growth and Interaction, Ph. D. Thesis, Division of Engineering, Brown University.

HANCOCK, J. W. and BROWN, D. K. 1983 — J. Mech. Phys. Solids, 31, 1.

HANCOCK, J. W. and MACKENZIE, A. C. 1976 — J. Mech. Phys. Solids, 24, 147.

NEEDLEMAN, A. and RICE, J. R. 1978 — Mechanics of Sheet Metal Forming, (ed. D. P. Koistinen and N. M. Wang), 237.

PEIRCE, D., ASARO, R. J. and NEEDLEMAN, A. 1982 — Acta Metall. 30, 1087.

PEIRCE, D., ASARO, R. J. and NEEDLEMAN, A. 1983 — Acta Metall. 31, 1951.

SAJE, M., PAN, J. and NEEDLEMAN,A. 1982 — Int. J. Fract. 19, 163.

TVERGAARD, V. 1981 — Int. J. Fract., 17, 389.

TVERGAARD, V. 1982 — J. Mech. Phys. Solids, 30, 399.

TVERGAARD, V. and NEEDLEMAN,A. 1984 — Acta Metall., 32, 157.

TVERGAARD, V., NEEDLEMAN, A. and LO, K.K. 1981 — J. Mech. Phys. Solids., 29, 115.

WILSON, M. L., HAWLEY, R. H. and DUFFY, J. 1980 — Engineering Fracture Mechanics 13, 371.

5. SCIENTIFIC PERSONNEL SUPPORTED BY THE GRANT

R.J. Asaro	Co-Investigator
W. Barron	Undergraduate Research Assistant
R.J. Clifton	Principal Investigator
H. Couque	Research Assistant (Sc.M. 6/84)
J. Duffy	Co-Investigator
L.B. Freund	Co-Investigator
K. Hartley	Research Assistant
R. Hawley	Research Engineer
R. Klopp	Research Assistant (Sc.M. 6/84)
G.L. LaBonte, Jr.	Technical Assistant
G. Majda	Faculty Associate
A. Molinari	Visiting Research Associate
A. Needleman	Co-Investigator
G. Ravichandran	Research Assistant (Sc.M. 6/83)
P. Rush	Technical Assistant
T. Shawki	Research Assistant (Sc.M. 6/83)
M. Toulios	Post Doctoral Research Associate
Wu, F.H.	Research Assistant (Ph.D. 6/83)
W. Yang	Research Assistant (Ph.D. 6/85)

END

FILMED

5-85

DTIC